2011

The spatial distribution of solar radiation under a melting Arctic sea ice cover

Karen E. Frey
Clark University, kfrey@clarku.edu

Donald K. Perovich
U.S. Army Cold Regions Research and Engineering Laboratory

Bonnie Light
University of Washington

The spatial distribution of solar radiation under a melting Arctic sea ice cover

Karen E. Frey,[1] Donald K. Perovich,[2,3] and Bonnie Light[4]

Received 25 August 2011; revised 17 October 2011; accepted 18 October 2011; published 18 November 2011.

[1] The sea ice cover of the Chukchi and Beaufort Seas is currently undergoing a fundamental shift from multiyear ice to first-year ice. Field observations of sea ice physical and optical properties were collected in this region during June–July 2010, revealing unexpectedly complex spatial distributions of solar radiation under the melt-season ice cover. Based on our optical measurements of first-year ice, we found the under-ice light field in the upper ocean to be spatially heterogeneous and dependent on wavelength, ice thickness, and the areal and geometric distribution of melt ponded and bare ice surfaces. Much of the observed complexity in radiation fields arose because the transmission of light through ponded ice was generally an order of magnitude greater than through bare, unponded ice. Furthermore, while many sites exhibited a consistent, exponential decay in light transmission through both ponded and bare ice surfaces, light transmission under bare ice was also observed to increase with depth (reaching maximum values ~5–10 m below the bottom of the ice). A simple geometric model shows these transmission peaks are a result of scattering in the ice and the interspersion of bare and ponded sea ice surfaces. These new observations of complex radiation fields beneath melt-season first-year sea ice have significant implications for biological production, biogeochemical processes, and the heat balance of sea ice and under-ice ocean waters and should be carefully considered when modeling these sea ice-related phenomena. **Citation:** Frey, K. E., D. K. Perovich, and B. Light (2011), The spatial distribution of solar radiation under a melting Arctic sea ice cover, *Geophys. Res. Lett.*, *38*, L22501, doi:10.1029/2011GL049421.

1. Introduction

[2] Some of the greatest changes to the Arctic sea ice cover are occurring in the Chukchi and Beaufort Seas. There has been a decrease in summer ice extent [*Serreze et al.*, 2007; *Stroeve et al.*, 2007; *Comiso et al.*, 2008] and thickness [*Kwok and Rothrock*, 2009], a change in the seasonality of melt and freeze-up [*Markus et al.*, 2009], and a shift from abundant perennial ice to predominantly seasonal ice [*Maslanik et al.*, 2007]. Several potential factors are contributing to this decline, including higher air temperatures [*Overland et al.*, 2008], changes in circulation patterns [*Nghiem et al.*, 2007; *Rampal et al.*, 2009], advection of ocean heat from lower latitudes [*Woodgate et al.*, 2006], changes in cloud conditions [*Francis et al.*, 2005; *Schweiger et al.*, 2008; *Kay et al.*, 2008], and enhanced solar heating of the upper ocean [*Wang and Key*, 2005; *Perovich et al.*, 2007, 2008; *Matsoukas et al.*, 2010].

[3] During summer, Arctic sea ice cover is a complex, evolving mosaic of ice, ponds, and open ocean. This morphological variability affects the reflection, absorption, and transmission of solar radiation in the ice-ocean system. There are large differences in light reflection from bare melting ice (65%), ponds of melt water (40%), and areas of open ocean (10%) [*Pegau and Paulson*, 2001; *Perovich et al.*, 2002]. The recent significant shifts from perennial to seasonal ice and the general ice thinning in the Chukchi and Beaufort Seas are reducing reflection of solar radiation by the ice cover (and thereby enhancing transmission of solar radiation into or through the ice). In turn, these changes are affecting the heat and mass balance of sea ice, as well as biological production and biogeochemical processes within and beneath the ice. For example, more light transmitted through the thinner and more ponded ice means more heat in the upper ocean available for melting on the underside of the ice or storage in the ocean. In addition, greater light transmittance may enhance primary productivity [e.g., *Gradinger*, 2009; *Mundy et al.*, 2009], reduce the nutritional quality of sea ice algae [*Leu et al.*, 2010], and/or increase the potential for UV photo-oxidation of dissolved organic matter and subsequent outgassing of CO_2 [e.g., *Minor et al.*, 2007; *Spencer et al.*, 2009].

[4] Previous work established that the variegated surface conditions of sea ice results in spatially variable albedo [*Hanesiak et al.*, 2001; *Perovich et al.*, 2002; *Grenfell and Perovich*, 2004] and light transmittance at the bottom of the ice [*Grenfell and Maykut*, 1977; *Perovich*, 1990; *Light et al.*, 2008]. However, the influence of a heterogeneous sea ice surface on the light field in the upper ocean under the ice was previously unknown. Here, in this study, we examine the light field under a summer first-year sea ice cover consisting of a mixture of bare and ponded sea ice surfaces. We present observations of the downwelling spectral light field at the base of the ice and in the upper ~50 m of the ocean water column. The complexity of the transmitted light is shown by a simple geometric model that is used to demonstrate the impact of ice surface conditions on the transmitted light field in the upper ocean.

2. Observations

[5] Field observations were made during the 2010 NASA ICESCAPE (Impacts of Climate change on the Ecosystems

[1]Graduate School of Geography, Clark University, Worcester, Massachusetts, USA.
[2]ERDC, Cold Regions Research and Engineering Laboratory, Hanover, New Hampshire, USA.
[3]Thayer School of Engineering, Dartmouth College, Hanover, New Hampshire, USA.
[4]Polar Science Center, University of Washington, Seattle, Washington, USA.

0094-8276/11/2011GL049421

Figure 1. Photograph of the first-year sea ice surface observed in the Chukchi Sea (71.93°N, 156.28°W) on 10 July 2010, highlighting the interspersion of bare and ponded ice surfaces. The two X locations denote the specific sites of the bare ice (black X) and melt pond (white X) field measurements.

and Chemistry of the Arctic Pacific Environment) cruise in the Chukchi and Beaufort Seas during June and July 2010 on the US Coast Guard Cutter *Healy*. The goal of this interdisciplinary program was to determine the impact of climate change on the biogeochemistry and ecology of the Chukchi and Beaufort Seas, which entailed characterizing the physical, biological, chemical, and optical properties of the ice and upper ocean during the time of year when solar radiation incident at the surface is at or near its peak. The characterization included measurements of ice thickness, melt pond depth, and the spectral reflection and transmission of light in the ice and in the upper ocean beneath the ice.

[6] The measurements reported in this study were made on 10 July 2010 on a first-year ice floe in the Chukchi Sea (71.93°N, 156.28°W) that was a mix of bare ice and mature melt ponds (Figure 1). The two X locations in Figure 1 denote the bare, unponded ice and melt pond locations where vertical profiles of light transmittance were measured from the surface ice cover to a depth of ~50 m in the water column. The bare ice was 1.27 m thick and the ponded ice was 0.83 m thick (with 0.15 m of ponded melt water on its surface).

[7] Spectral light transmittances were measured through the ice using an Analytical Spectral Devices dual detector spectroradiometer. The instrument has a wavelength range from 380 to 890 nm. One detector was used to monitor the incident solar irradiance, while the other measured transmitted irradiance. The transmitted sensor was placed under the ice using an articulated extension arm [*Light et al.*, 2008]. Transmittances through the ponded ice were roughly an order of magnitude larger than the bare ice (Figure 2). The peak transmittance was 0.46 at 425 nm for ponded ice and 0.034 at 520 nm for bare ice. In both bare and ponded ice cases, transmittances decreased sharply beyond 700 nm owing to increased absorption by the ice. By comparison, these first-year ice transmittances are much larger than what would be expected for multiyear ice [e.g., *Grenfell and Maykut*, 1977; *Light et al.*, 2008].

[8] Measurements of light transmittances beneath the ice through the water column below were collected at the same locations as the observations described above. A modified Compact-Optical Profiling System (C-OPS, Biospherical Instruments Inc.) cosine collector radiometer was lowered to a depth of ~50 m through an auger-drilled ~25 cm hole in the ice. At the bare ice surface site, the hole was re-filled with ice tailings to mimic the previously undisturbed bare ice surface. At the ponded ice surface site, the C-OPS was offset from the hole such that the cosine collector on the instrument looked directly up at the underside of the ice. Although minimal light contamination through the auger hole at the ponded ice surface site may be possible, the models presented by *Light et al.* [2008] show that any light through a 25 cm hole in the ice becomes negligible ~1 m below the bottom of the ice. The C-OPS collected downwelling irradiance with 19 channels (320, 340, 380, 395, 412, 443, 465, 490, 510, 532, 555, 560, 625, 665, 670, 683, 710, 780nm, and photosynthetically active radiation (PAR, 400–700nm)). An above-water surface reference simultaneously measured incident global irradiance with the same 19 channels. This surface reference was mounted at the top of a tripod (~2.5 m above the ice surface) that stood on the ice within ~1.5 m of where the C-OPS measurements were collected. The profiling C-OPS and surface reference instruments were utilized in concert to calculate the fractional light transmittance through the ice, accounting for any variability in solar conditions while the under-ice profiles were collected.

[9] Resulting profiles of light transmittances in the water column under the melt ponded and bare ice surfaces are plotted in Figure 3. Transmittances through the ponded ice surface (Figure 3a) start at the values measured at the underside of the ice and monotonically decrease with depth. The steepness of the drop-off is a function of wavelength and is primarily due to the spectral differences in the absorption coefficient of seawater. The decrease in transmittance with depth at each wavelength is well-fit by an exponential relationship (correlation coefficients greater than 0.99). The general shape of the observed depth dependence of transmittance is consistent with expected profiles for a water column with uniform optical properties.

[10] In contrast, the spectral transmittance profiles under the bare ice surface (Figure 3b) show the effects of a heterogeneous ice surface and the influence of relatively large light transmittance through adjacent melt ponded surfaces. Most spectral profiles show an initial increase with depth, peak transmittance at a ~5–10 m depth, followed by an exponential decrease with depth. For example, the transmitted downwelling irradiance at a wavelength of 465 nm increases by nearly a factor of three from the ice bottom to a depth of 10 m. However, at wavelengths longer than 625 nm (where absorption in the water is greater), there is no subsurface maximum in the water column below the ice and light transmittance decreases with depth over the entire profile. This is the pattern of light transmission with depth that would have been expected for all wavelengths. While the patterns in transmitted irradiance profiles described above are readily apparent, there are also more subtle characteristics of the profiles. For example, slight shifts in transmitted irradiance at depths of ~40 m under both ponded and bare ice (particularly evident in the inset semi-log plots) (Figure 3) are associated with peaks in chlorophyll-*a* concentrations at this depth observed through profiling fluorometer measurements.

[11] Our measurements of peak transmittances at depths ~5–10 m below the bottom of the ice at this site (observed at most wavelengths) was unexpected and difficult to explain in terms of the properties of the water column. For the case

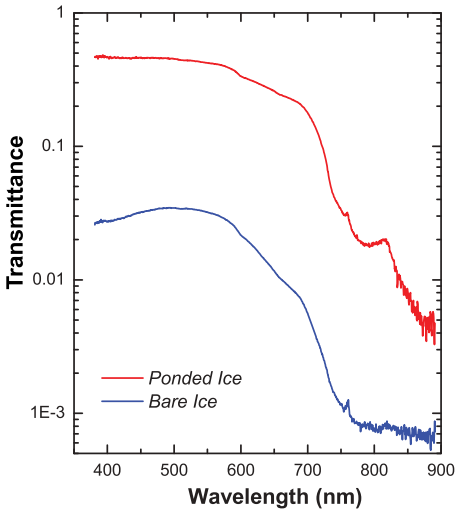

Figure 2. Transmittance measured directly beneath ponded ice and bare ice for horizontally homogenous conditions.

of a uniform ice cover and an optically homogeneous water column, light transmission at a particular wavelength would be expected to follow a simple exponential decay. If optical properties in the water column varied with depth, the transmitted light field could exhibit changing rates of decline, but not an increase in magnitude as was observed here. We believe this observed peak in transmitted light is due to horizontal propagation of radiation transmitted by adjacent melt ponded ice surfaces. As Figure 1 shows, the surface is a mosaic of bare ice, melt ponds, and areas of open water. As such, moving downward in the water column from the ice-water interface, an upward looking sensor will see an evolving mix of bare ice, ponded ice, and open water. The depth dependence of light transmittance will be a combination of the changing view and extinction of light in the water column. In the following section, we apply a simple geometric optical model to explore the influence of ice surface conditions on the transmitted light field in the water column under a bare ice surface in the vicinity of melt ponded ice surfaces.

3. A Simple Geometric Model

[12] With some simplifying assumptions, it is possible to formulate an expression for transmitted irradiance as a function of depth under a spatially heterogeneous ice cover. Here, we formulate a simple geometric model of light transmittance below an area of bare ice in the vicinity of melt ponded surfaces. Assumptions about the ice morphology are that the ice is of uniform thickness, the ponds are of uniform depth, the pond areal fraction is P, there is axial symmetry in the distribution of ponds and bare ice, and the observation site is centered at a site of bare ice with horizontal radius R. In terms of optical properties, we assume that the transmitted light field under the ice is independent with respect to the azimuth angle and the irradiance

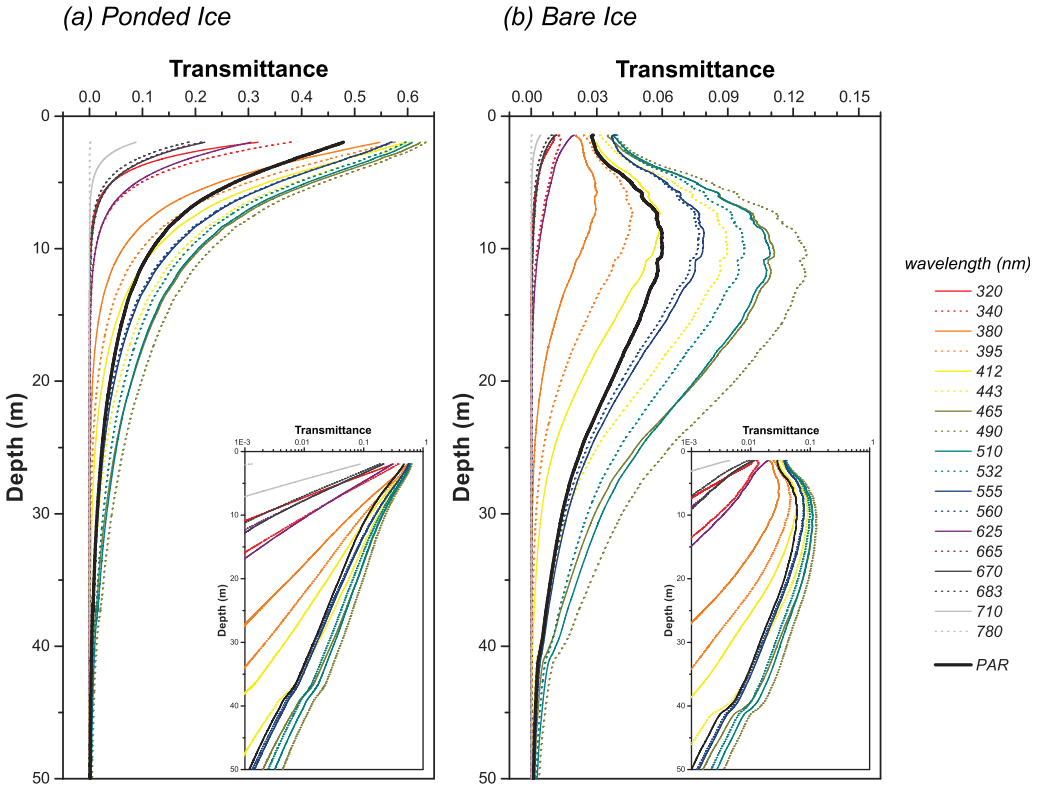

Figure 3. Transmittance at selected wavelengths (in nm) as well as photosynthetically active radiation (PAR) measured in the water column under (a) ponded ice and (b) bare ice surfaces. The inset plots show the relationships in semi-log form. The ponded ice case (which follows a typical exponential decay) shows the vertical profiles as straight lines in semi-log form, whereas the bare ice case does not (since transmittance peaks at depths of ~5–10 m).

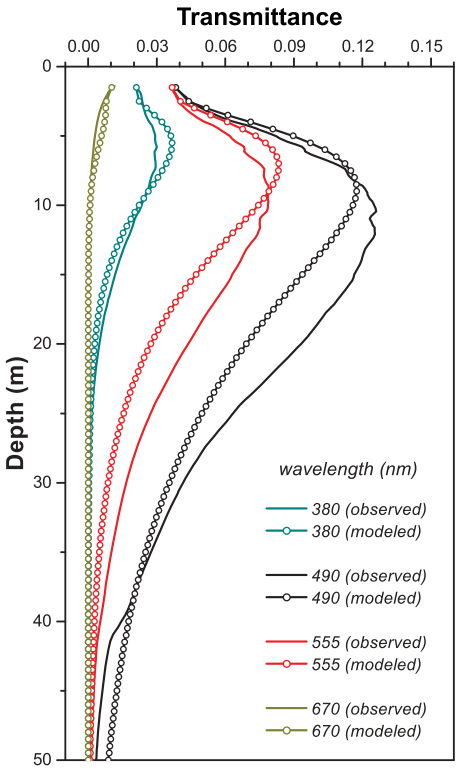

Figure 4. Modeled and observed transmittance in the water column under the bare ice case at 380, 490, 555, and 670 nm.

extinction in the water column is exponential with a coefficient of k. Directly at the bottom of the ice, the transmitted radiance through the bare ice is defined as I, whereas the radiance through the ponded ice is defined as $N \cdot I$.

[13] The general expression for the irradiance (F) is given as:

$$F(z) = \int_0^{2\pi} \int_0^{\pi/2} I(\theta, \varphi) \cos\theta \ \sin\theta \ d\theta \ d\varphi \qquad (1)$$

where θ is the zenith angle and φ is the azimuth angle. Equation (1) can be separated into contributions from both bare ice and ponded sea ice surfaces. By applying the assumptions stated above, the total combined irradiance as a function of depth (z) under the bare ice is:

$$F_{total}(z) = \pi I\left[1 + P(N-1)\cos^2\theta_i\right]e^{-kz} \qquad (2)$$

where $\theta_i = arctangent\ (R/z)$. The irradiance at depth depends on (i) pond fraction and the bare ice area in vicinity of the measurement sites; (ii) the amount of light transmitted through the ice and melt ponds; and (iii) the extinction coefficient of seawater beneath the ice. The auxiliary material presents the full derivation of equation (2).[1]

[14] We evaluated equation (2) for four wavelengths (380, 490, 555, and 670 nm), each exhibiting various degrees of influence by adjacent melt ponded ice surfaces (Figure 3b). Light transmittance at 490 nm exhibited the greatest sub-surface transmittance peak (~10 m below the bottom of the ice), whereas transmittance at 670 nm contrastingly decreased monotonically with an expected transmittance peak highest in the water column (at the ice-water interface directly below the ice). Observations are used to define the input parameters for equation (2). Analysis of Figure 1 showed a pond fraction (P) of 0.5 and a central bare ice radius (R) of 5 m. Values for N at each wavelength were determined from the transmittances in Figure 2, whereas values for I at each wavelength were determined from transmittances directly below the ice as shown in Figure 3b. Extinction coefficients in the water column (k) were estimated by applying an exponential fit to the 15–25 m portion of the transmittance curves in Figure 3a. This central portion was selected to avoid the ice morphology effects of the upper portion of the water column and the small light levels of the lower portion. The exponential fit was excellent (with correlation coefficients greater than 0.999), with absorption coefficients of 0.228 m^{-1} at 380 nm, 0.070 m^{-1} at 490 nm, 0.119 m^{-1} at 555 nm, and 0.54 m^{-1} at 670 nm.

[15] Figure 4 compares observed and modeled transmittance profiles in the upper 50 m of the water column. At 380, 490, and 555 nm, the modeled transmittance profiles agree closely with observations, producing distinct peaks at the appropriate depths (~5–10 m), and then decaying with greater depths. While the modeled peak transmittances are slightly shallower than that observed, the general form of the transmittance profiles are similar. In contrast to the 380, 490, and 555 nm profiles, a transmittance peak at a depth below the ice-water interface is not found for 670 nm in either observed or modeled transmittances owing to a large amount of absorption in the water column at this wavelength. These comparisons support the hypothesis that transmitted irradiance profiles in the water column under the ice are governed by a combination of both surface ice conditions and overall extinction in the water column beneath the ice. We believe that the slight differences between observed and modeled profiles may result from a surface distribution of ponded and bare ice that is more complex than is able to be modeled here. A more detailed two-dimensional radiative transfer treatment could address this issue.

4. Implications and Conclusions

[16] During the 2010 ICESCAPE cruise, light transmission measurements were made at 10 different ice floes distributed throughout the Chukchi Sea. Transmission peaks at depth were observed at two of these floes, but more certainly would have been observed had selected bare ice sites been located in closer proximity to melt ponded ice surfaces. The field observations and equation (2) provide insight into the factors governing these unexpectedly complex light transmittance profiles. More specifically, a transmittance peak at depth occurs (i) under bare ice, but not ponds; (ii) when there is much higher transmittance through ponded ice than bare ice; (iii) when the pond fraction is large (>0.4) and the bare ice is distributed in small (<10 m) patches; and (iv) at wavelengths where absorption in ice and water are small. Increasing the pond fraction and pond transmittance enhance the magnitude of the transmittance peak at depth beneath bare ice surfaces. Increasing the size of the ice area (R) decreases the magnitude of the peak and shifts it even deeper in the water column. Larger water extinction coefficients reduce the magnitude, and if large enough, eliminate the transmittance peak at depth altogether. Even though a sub-surface transmittance peak

[1]Auxiliary materials are available in the HTML. doi:10.1029/2011GL049421.

may not be apparent, the variegated surface of bare ice, ponds, and leads may still significantly affect the transmitted light field beneath the ice.

[17] The transmission peak at depth below the ice-water interface investigated here occurs owing to scattering in the ice and to a lesser extent in ocean waters as well. This results in the horizontal propagation of light and leads to unexpectedly high light transmittance under bare ice surfaces in the vicinity of melt ponds. If the propagation were strictly vertical, shafts of enhanced light intensity would reach directly beneath the melt ponds and would be detectable beneath these ponds only. A two-dimensional radiative transfer model is needed to represent the full spatial distribution of propagated light under non-idealized surface conditions.

[18] The observations and model presented in this study demonstrate that the solar irradiance field in the upper ocean under a melting first-year sea ice cover varies both vertically and horizontally. Our results indicate that the greatest variation in light transmission occurs just below the bottom of the ice (e.g., where bare ice and ponded ice may differ by a factor up to ~13.2 at 490 nm for the specific site investigated here). However, the pond:bare ice transmission ratio decreases asymptotically with depth, with a ratio of ~1.8 at 490 nm at the transmission peak ~10 m below the ice bottom. At a ~20 m depth below the ice bottom, transmission becomes nearly independent of variable surface ice conditions and exhibits a pond:bare ice transmission ratio of ~1.05 at 490 nm. Owing to the relative motion of the ice, the transmitted irradiance in the upper ocean is constantly changing as bare ice and melt ponds pass over ocean waters. This has important implications not only for solar heating of ocean waters beneath the ice, but also for the potential light available for primary production and biogeochemical processes below the ice. For example, for phytoplankton adapted to a particular range of light levels, the depth of the transmission peak offers a location with relatively large light levels resulting from the proximity of melt ponds. These unexpected complexities in the transmitted light fields below melt season sea ice are critical to consider when modeling the potential physical, biological, and biogeochemical impacts of melt ponded ice surfaces on the under-ice ocean water column.

[19] **Acknowledgments.** This research was part of the NASA Impacts of Climate change on the Ecosystems and Chemistry of the Arctic Pacific Environment (ICESCAPE) project with support from the NASA Cryospheric Sciences Program (Grant #NNX10AH71G to K. Frey and Grant #NNH10A017IE to D. Perovich and B. Light) and the NASA Ocean Biology and Biogeochemistry Program. The field component of this research would not have been possible without the tremendous support from the commanding officer, marine science technicians, crew, and officers of USCGC *Healy* on the HLY1001 mission to the Chukchi Sea in June–July 2010. We also thank Lee Brittle, Ruzica Dadic, Christopher Polashenski, Luke Trusel, and Christie Wood for their support with field measurements. Lastly, we thank two anonymous reviewers for their constructive comments and suggestions.

[20] The Editor thanks Mark Tschudi and an anonymous reviewer for their assistance in evaluating this paper.

References

Comiso, J. C., C. L. Parkinson, R. Gersten, and L. Stock (2008), Accelerated decline in the Arctic sea ice cover, *Geophys. Res. Lett.*, *35*, L01703, doi:10.1029/2007GL031972.

Francis, J. A., E. Hunter, J. R. Key, and X. Wang (2005), Clues to variability in Arctic minimum sea ice extent, *Geophys. Res. Lett.*, *32*, L21501, doi:10.1029/2005GL024376.

Gradinger, R. (2009), Sea-ice algae: Major contributors to primary production and algal biomass in the Chukchi and Beaufort Seas during May/June 2002, *Deep Sea Res., Part II*, *56*, 1201–1212, doi:10.1016/j.dsr2.2008.10.016.

Grenfell, T. C., and G. A. Maykut (1977), The optical properties of ice and snow in the Arctic Basin, *J. Glaciol.*, *18*, 445–463.

Grenfell, T. C., and D. K. Perovich (2004), The seasonal evolution of albedo in a snow-ice-land-ocean environment, *J. Geophys. Res.*, *109*, C01001, doi:10.1029/2003JC001866.

Hanesiak, J. M., D. G. Barber, R. A. DeAbreau, and J. J. Yackel (2001), Local and regional albedo observations of arctic first year sea ice during melt ponding, *J. Geophys. Res.*, *106*(C1), 1005–1016, doi:10.1029/1999JC000068.

Kay, J. E., T. L'Ecuyer, A. Gettelman, G. Stephens, and C. O'Dell (2008), The contribution of cloud and radiation anomalies to the 2007 Arctic sea ice extent minimum, *Geophys. Res. Lett.*, *35*, L08503, doi:10.1029/2008GL033451.

Kwok, R., and D. A. Rothrock (2009), Decline in Arctic sea ice thickness from submarine and ICESat records: 1958–2008, *Geophys. Res. Lett.*, *36*, L15501, doi:10.1029/2009GL039035.

Leu, E., J. Wiktor, J. E. Soreide, J. Berge, and S. Falk-Peterson (2010), Increased irradiance reduced food quality of sea ice algae, *Mar. Ecol. Prog. Ser.*, *411*, 49–60, doi:10.3354/meps08647.

Light, B., T. C. Grenfell, and D. K. Perovich (2008), Transmission and absorption of solar radiation by Arctic sea ice during the melt season, *J. Geophys. Res.*, *113*, C03023, doi:10.1029/2006JC003977.

Markus, T., J. C. Stroeve, and J. Miller (2009), Recent changes in Arctic sea ice melt onset, freezeup, and melt season length, *J. Geophys. Res.*, *114*, C12024, doi:10.1029/2009JC005436.

Maslanik, J. A., C. Fowler, J. Stroeve, S. Drobot, J. Zwally, D. Yi, and W. Emery (2007), A younger, thinner Arctic ice cover: Increased potential for rapid, extensive sea-ice loss, *Geophys. Res. Lett.*, *34*, L24501, doi:10.1029/2007GL032043.

Matsoukas, C., N. Hatzianastassiou, A. Fotiadi, K. G. Pavlakis, and I. Vardavas (2010), The effect of Arctic sea-ice extent on the absorbed (net) solar flux at the surface, based on ISCCP-D2 cloud data for 1983–2007, *Atmos. Chem. Phys.*, *10*, 777–787, doi:10.5194/acp-10-777-2010.

Minor, E. C., B. L. Dalzell, A. Stubbins, and K. Mopper (2007), Evaluating the photoalteration of estuarine dissolved organic matter using direct temperature-resolved mass spectrometry and UV-visible spectroscopy, *Aquat. Sci.*, *69*(4), 440–455, doi:10.1007/s00027-007-0897-y.

Mundy, C. J., et al. (2009), Contribution of under-ice primary production to an ice-edge upwelling phytoplankton bloom in the Canadian Beaufort Sea, *Geophys. Res. Lett.*, *36*, L17601, doi:10.1029/2009GL038837.

Nghiem, S. V., I. G. Rigor, D. K. Perovich, P. Clemente-Colón, J. W. Weatherly, and G. Neumann (2007), Rapid reduction of Arctic perennial sea ice, *Geophys. Res. Lett.*, *34*, L19504, doi:10.1029/2007GL031138.

Overland, J. E., M. Wang, and S. Salo (2008), The recent Arctic warm period, *Tellus, Ser. A*, *60*, 589–597, doi:10.1111/j.1600-0870.2008.00327.x.

Pegau, W. S., and C. A. Paulson (2001), The albedo of Arctic leads in summer, *Ann. Glaciol.*, *33*, 221–224, doi:10.3189/172756401781818833.

Perovich, D. K. (1990), Theoretical estimates of light reflection and transmission by spatially complex and temporally varying sea ice covers, *J. Geophys. Res.*, *95*(C6), 9557–9567, doi:10.1029/JC095iC06p09557.

Perovich, D. K., T. C. Grenfell, B. Light, and P. V. Hobbs (2002), Seasonal evolution of the albedo of multiyear Arctic sea ice, *J. Geophys. Res.*, *107*(C10), 8044, doi:10.1029/2000JC000438.

Perovich, D. K., B. Light, H. Eicken, K. F. Jones, K. Runciman, and S. V. Nghiem (2007), Increasing solar heating of the Arctic Ocean and adjacent seas, 1979–2005: Attribution and role in the ice-albedo feedback, *Geophys. Res. Lett.*, *34*, L19505, doi:10.1029/2007GL031480.

Perovich, D. K., J. A. Richter-Menge, K. F. Jones, and B. Light (2008), Sunlight, water, and ice: Extreme Arctic sea ice melt during the summer of 2007, *Geophys. Res. Lett.*, *35*, L11501, doi:10.1029/2008GL034007.

Rampal, R., J. Weiss, and D. Marsan (2009), Positive trend in the mean speed and deformation rate of Arctic sea ice, 1979–2007, *J. Geophys. Res.*, *114*, C05013, doi:10.1029/2008JC005066.

Schweiger, A. J., J. Zhang, R. W. Lindsay, and M. A. Steele (2008), Did unusually sunny skies help drive the record sea ice minimum of 2007?, *Geophys. Res. Lett.*, *35*, L10503, doi:10.1029/2008GL033463.

Serreze, M. C., M. M. Holland, and J. Stroeve (2007), Perspectives on the Arctic's shrinking sea-ice cover, *Science*, *315*, 1533–1536, doi:10.1126/science.1139426.

Spencer, R. G. M., et al. (2009), Photochemical degradation of dissolved organic matter and dissolved lignin phenols from the Congo River, *J. Geophys. Res.*, *114*, G03010, doi:10.1029/2009JG000968.

Stroeve, J., M. M. Holland, W. Meier, T. Scambos, and M. Serreze (2007), Arctic sea ice decline: Faster than forecast, *Geophys. Res. Lett.*, *34*, L09501, doi:10.1029/2007GL029703.

Wang, X., and J. R. Key (2005), Arctic surface, cloud, and radiation properties based on the AVHRR Polar Pathfinder dataset. Part II: Recent trends, *J. Clim.*, *18*, 2575–2593, doi:10.1175/JCLI3439.1.

Woodgate, R. A., K. Aagaard, and T. J. Weingartner (2006), Interannual changes in the Bering Strait fluxes of volume, heat and freshwater between 1991 and 2004, *Geophys. Res. Lett.*, *33*, L15609, doi:10.1029/2006GL026931.

K. E. Frey, Graduate School of Geography, Clark University, Worcester, MA 01610, USA. (kfrey@clarku.edu)

B. Light, Polar Science Center, University of Washington, Seattle, WA 98105, USA.

D. K. Perovich, ERDC, Cold Regions Research and Engineering Laboratory, Hanover, NH 03755, USA.